Modulation of intratumoral hypoxia by the epidermal growth factor receptor inhibitor gefitinib detected using small animal PET imaging

Benjamin Solomon,[1,3] David Binns,[2] Peter Roselt,[2] Leonard I. Weibe,[4] Grant A. McArthur,[1,3] Carleen Cullinane,[3] and Rodney J. Hicks[2,3]

[1]Research Division and [2]Department of Molecular Imaging, Peter MacCallum Cancer Centre; [3]Department of Medicine, St Vincent's Hospital, Melbourne, Australia; and [4]Faculty of Pharmacy and Pharmaceutical Sciences, University of Alberta, Edmonton, Alberta, Canada

Abstract

Blockade of signaling through the epidermal growth factor receptor (EGFR) tyrosine kinase by inhibitors such as gefitinib (Iressa) can inhibit tumor angiogenesis and enhance responses to ionizing radiation. In this study, the ability of gefitinib to modulate intratumoral oxygenation was evaluated in human EGFR-expressing A431 squamous cell carcinoma xenografts using *in vivo* small animal positron emission tomography (PET) imaging with the hypoxia marker [^{18}F]fluoroazomycin arabinoside (FAZA) and by the immunohistochemical detection of hypoxia-induced adducts of the 2-nitroimidazole, pimonidazole. Serial noninvasive PET imaging of A431 xenografts showed a significant reduction in FAZA uptake following treatment with 75 mg/kg/d of gefitinib [tumor to background ratio, 6.1 $\pm$ 1.0 (pretreatment) versus 2.3 $\pm$ 0.6 (posttreatment); $P = 0.0004$]. Similarly, *ex vivo* quantitation of FAZA uptake showed significantly reduced FAZA uptake in established A431 xenografts treated with gefitinib compared with vehicle control (tumor to blood ratio for controls versus gefitinib, 8.0 $\pm$ 3.0 versus 2.7 $\pm$ 0.8; $P = 0.007$; or tumor to muscle ratio controls versus gefitinib, 8.6 $\pm$ 2.8 versus 2.6 $\pm$ 1.0; $P = 0.002$). The effect of gefitinib treatment seemed to be independent of tumor size. In addition, gefitinib treatment reduced pimonidazole-binding in A431 xenografts measured after 5 and 8 days of gefitinib treatment compared with baseline and with tumors treated with vehicle alone. A strong correlation was observed between pimonidazole binding and FAZA uptake. Together, these findings show that gefitinib reduces intratumoral hypoxia. [Mol Cancer Ther 2005;4(9):1417–22]

Introduction

Hypoxia in human tumors is a poor prognostic feature that is associated with an aggressive clinical and biological phenotype (1). The hypoxic microenvironment within tumors promotes both local invasion and distant metastasis (1, 2) and is associated with resistance to anticancer therapies, in particular, ionizing radiation (3). Methods to reduce hypoxia in tumors may therefore represent potentially valuable adjunctive therapeutic approaches.

Gefitinib (Iressa or ZD1839) is an orally active, reversible inhibitor of the epidermal growth factor receptor tyrosine kinase (4). It is well-tolerated and shows clinical activity in a variety of tumor types including non–small cell lung cancer and head and neck squamous cell carcinoma (5). In preclinical studies, gefitinib and other epidermal growth factor receptor inhibitors have shown the ability to potentiate the effects of ionizing radiation (6–9).

[^{18}F]Fluoroazomycin arabinoside (FAZA) is an arabinose sugar–coupled 2-nitroimidazole derivative that undergoes an oxygen-reversible one-electron reduction in hypoxic environments to form active radicals that bind covalently to cellular macromolecules. FAZA has been shown to be a hypoxia-specific imaging agent with potentially superior biokinetic properties to the standard hypoxia tracer, fluoromisonidazole (10). In this study, the ability of gefitinib to modulate oxygenation in human epidermal growth factor receptor expressing A431 squamous cell carcinoma xenografts was examined using *in vivo* small animal positron emission tomography (PET) imaging with FAZA. Results of the *in vivo* FAZA imaging were confirmed by immunohistochemical detection of adducts of the 2-nitroimidazole, pimonidazole.

Materials and Methods

Reagents

Gefitinib (AstraZeneca, Macclesfield, United Kingdom) was provided as a micronized powder and suspended in 0.5% Tween 80 in water for administration to mice at a dose of 75 mg/kg/d by i.p. injection. Pimonidazole (NPI, Belmont, MA) was dissolved in 0.9% saline and given at a concentration of 60 mg/kg via tail vein injection to mice. The radiotracer FAZA ([^{18}F]1-α-D-(5-fluoro-5-deoxy-arabinofuranosyl)-2-nitroimidazole) was synthesized from

Received 3/9/05; revised 5/15/05; accepted 6/20/05.

Grant support: B. Solomon was sponsored by a medical postgraduate scholarship from the National Health and Medical Research Council.

The costs of publication of this article were defrayed in part by the payment of page charges. This article must therefore be hereby marked advertisement in accordance with 18 U.S.C. Section 1734 solely to indicate this fact.

Requests for reprints: Rodney J. Hicks, Peter MacCallum Cancer Institute, Locked Bag 1, A'Beckett Street, Melbourne 8006, Australia. Phone: 61-3-9656-1852; Fax: 61-3-9656-1826. E-mail: Rod.Hicks@petermac.org

doi:10.1158/1535-7163.MCT-05-0066

the precursor 1-(2,3-diacetyl-5-tosyloxy-α-D-arabinofuranosyl)-2-nitroimidazole using a modification of the nucleophilic fluorination method of Reischl et al. (11). Briefly, [^{18}F]-fluoride was obtained through the ^{18}O(p,n)^{18}F nuclear reaction by bombarding [^{18}O]-enriched (>90%) water with 12 MeV protons using the Oxford Scientific OSCAR 7 cyclotron (Oxford Instruments, Oxford, United Kingdom). Using the coincidence FDG synthesizer (GE Medical Systems, Milwaukee, WI), [^{18}F]-fluoride was isolated, conditioned with Kryptofix 222/K_2CO_3, and azeotropically dried before reaction with precursor dissolved in acetonitrile. The resulting fluorinated intermediate was then isolated by solid phase extraction using a tC18 column and washed with water. The tC18-trapped intermediate was treated with 0.1 N NaOH and FAZA subsequently eluted using citrate buffer. FAZA then was purified by semi-preparative high-performance liquid chromatography using Phenomenex Luna C18(2) (5 μm, 50 × 10 mm) and Phenomenex Nucleosil C18 (5 μm, 250 × 10 mm) columns connected in series, and a mobile phase consisting of 8% ethanol in 0.9% saline. Isolated FAZA was passed through a 0.22-μm filter into sterile vials. Radiochemical purity of the final product was >98%.

A431 Tumor Xenografts

Athymic nude mice (BALB/c nude, 8–12 weeks old) were obtained from the Animal Resources Centre (Perth, Western Australia) and housed in microisolator boxes. Institutional animal ethics committee approval was obtained for all experiments. Xenografts were established by injecting 3×10^6 exponentially growing A431 cells (American Type Culture Collection) in 50 μL PBS into the s.c. tissue above the right forelimb of anaesthetized mice. Experiments were done when tumors had reached a size of 200 mm^3.

PET Imaging

PET imaging was done using a dedicated small animal PET scanner (Mosaic, Philips, Cleveland, OH). The scanner was one of two prototype, preproduction units, the performance characteristics of which have recently been described (12). In brief, the scanner has an effective axial field of view of 11.6 cm and resolution measured at 2.26 mm at the center of the field of view. On the basis of previous biodistribution studies conducted in nude mice bearing A431 xenografts (10), PET scan acquisition was started 3 hours after administration of ~500 μCi of FAZA given by tail vein injection. A static 15-minute scan was obtained with the mouse immobilized and anaesthetized in a container into which 2% isoflurane gas was mixed in equal parts with oxygen and air, delivered at a total rate of 400 mL/min. A single bed position acquisition was sufficient to encompass the whole of the body of the mouse. Attenuation correction, either measured or estimated, was not done. Scans were acquired in a three-dimensional volume mode, and rebinned into two-dimensions using the Fourier rebinning algorithm. The data were reconstructed using the ordered subset expectation maximization technique (four iterations and eight subsets) into 1-mm transaxial slices.

Image analysis and calculation of tumor to background ratio were done on transaxial images by determining the maximal and mean uptake within user-defined regions representing the tumor and the background, respectively. The tumor to background ratio was calculated as the maximal count in the tumor region divided by the mean count in the background region. Values from three serial transaxial sections at the midtumor plane were obtained and averaged to determine the tumor to background ratio for each tumor. For *ex vivo* quantitation of FAZA uptake, ~500 μL of blood was obtained by a cardiac bleed of an anaesthetized mouse and tumor and muscle from the thigh were obtained by dissection immediately postmortem. The blood and a preweighed amount of muscle and whole tumors were placed in 10 mL flat-bottomed tubes. Counts were determined by placing tubes in a well counter attached to a multichannel analyzer (187-950-A100 MCA, Biodex Medical Systems, Shirley, NY) interfaced with Atomlab 950 software (Biodex Medical Systems). Counts with an energy of 511 keV (±15%) were quantified, and expressed as counts per minute (cpm). Tumor/blood ratio (w/v) and tumor/muscle (w/w) were calculated using the formula $(T_c/T_w) / (B_c/B_v)$ and $(T_c/T_w) T_w) / (M_c/M_w)$, respectively [where T_c = tumor count (cpm); T_w = tumor weight (g); B_c = blood count (cpm); B_v = blood volume (mL); M_c = muscle count (cpm); and M_w = muscle weight (g)].

Immunohistochemistry for Pimonidazole Adducts

For pimonidazole immunohistochemistry, 60 mg/kg of pimonidazole (NPI) was given via tail vein injection to mice bearing A431 tumor xenografts. Three hours later, tumors were harvested, dissected into two or three portions and fixed with 10% neutral buffered formalin overnight and embedded in paraffin. Sections (4 μm thick) were incubated in an Autostainer with hypoxyprobe Mab (NPI) that had been previously biotinylated for 30 minutes using the Animal Research Kit (DAKO, Carpinteria, CA) according to the manufacturer's instructions. Slides were then incubated with Streptavidin (DAKO) for 10 minutes. After washing, aminoethylcarbozole chromogen (AEC+, DAKO) was applied for 10 minutes. Sections were counterstained in hematoxylin, rinsed, mounted with an aqueous mount (DAKO ultramount) and dried on a hot plate before coverslipping with DPX. Quantitation of pimonidazole binding was done on low magnification (4×) digital photomicrographs of the entire stained section of tumors (two or three sections per tumor) acquired using a SPOT RT slider cooled digital camera coupled to a Zeiss Axioskope 2 microscope. Using image analysis software (SPOT version 3.5, Diagnostic Instruments Inc., Sterling Heights, MI), the area of pimonidazole-positive tissue, the total area of the tumor section and the area of necrotic tissue in the tumor was determined. The percentage of pimonidazole binding was defined as: 100 × pimonidazole-positive area / (total tumor area − necrotic area). Three different tumors were examined for each treatment group and time point by an observer blinded to the treatment allocation of the tumor.

Statistics

Unpaired t tests were used for comparisons between groups of tumors and paired t tests for comparisons within individual tumors before and after treatment and were calculated using SigmaStat software (SPSS, Chicago, IL). All t tests were two-sided.

Results

Initial characterization of the effects of gefitinib on hypoxia in A431 xenografts was done by *in vivo* PET imaging using the recently validated hypoxia marker FAZA (10) and by *ex vivo* measurement of FAZA uptake into tumors. Using a dedicated small animal PET scanner, serial noninvasive FAZA PET imaging was done on established A431 xenografts, immediately before and after five daily treatments with 75 mg/kg/d gefitinib. Significant baseline FAZA uptake was evident in all tumors (tumor to background ratio, 6.1 ± 1.0). Following five daily treatments with gefitinib, although the size of the tumors had not significantly changed (410 ± 100 mm^3 pretreatment compared with 373 ± 110 mm^3 posttreatment; P value = 0.55), the FAZA uptake in the tumors was both qualitatively and quantitatively reduced compared with baseline (tumor to background ratio, 2.3 ± 0.6) as shown in Fig. 1. This difference was highly statistically significant by paired t test ($P = 0.0004$).

A second cohort of mice with established s.c. A431 xenografts was treated with 75 mg/kg/d of gefitinib or vehicle control (0.5% Tween 80) for 5 days. Mice were then injected with FAZA and imaged after 3 hours using a small animal PET scanner. As seen in Fig. 2, there was greater FAZA uptake apparent in A431 tumors in mice treated with vehicle (left) than in tumors from mice treated with gefitinib (right). Immediately following the PET imaging, mice were sacrificed and tumors, blood, and muscle were harvested for *ex vivo* quantitation of FAZA uptake. The average tumor to blood ratio for the control xenografts (vehicle-treated) was significantly higher than that for the gefitinib-treated tumors [controls versus gefitinib, 8.0 ± 3.0 versus 2.7 ± 0.8 (mean ± SD); $P = 0.007$]. Similarly, the average tumor to muscle ratios for the control xenografts was significantly higher than that for the gefitinib-treated tumors [controls versus gefitinib, 8.6 ± 2.8 versus 2.6 ± 1.0 (mean ± SD); $P = 0.002$].

To investigate the possibility that increasing tumor size may be associated with increasing hypoxia within A431 xenografts, and hence may confound interpretation of the effect of gefitinib, the relationship between tumor size and FAZA uptake was determined. The size of untreated A431 tumors (as reflected by tumor mass) was compared with the tumor to blood ratios and the tumor to muscle ratios of FAZA uptake. No correlation was observed between tumor mass and FAZA tumor to blood ratio ($r^2 = 0.01$) or between tumor mass and FAZA tumor to muscle ratio ($r^2 = 0.05$) as shown in Fig. 3. These data suggest that, at least for the size range of tumors used in this study, there was no significant correlation between increasing tumor size and FAZA uptake.

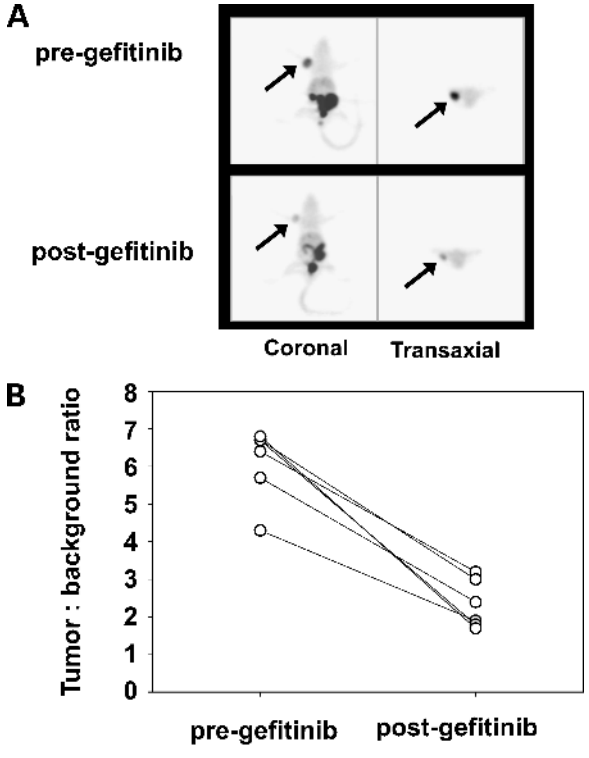

Figure 1. Effect of gefitinib treatment on baseline hypoxia in A431 xenografts. **A,** FAZA PET imaging was done on BALB/c nude mice with established A431 xenografts at baseline and after 5 d of treatment with 75 mg/kg/d of gefitinib ($n = 6$). Representative images are shown before and after treatment with gefitinib (*arrows*, tumors). **B,** tumor to background ratios for FAZA avidity at day 1 (pretreatment) and at day 5. A significant reduction in FAZA tumor to background ratio was seen (pretreatment versus posttreatment, 6.1 ± 1.0 versus 2.3 ± 0.6; $P = 0.0004$).

To further validate the effects of gefitinib on tumor hypoxia, immunohistochemical detection of hypoxia-induced adducts of pimonidazole was done (Fig. 4A). Pimonidazole, like other 2-nitroimidazole compounds, undergoes a nitroreductase catalyzed single-electron reduction, and binds covalently to macromolecular cellular components in hypoxic cells (13). As pimonidazole adducts are readily detectable by immunohistochemical techniques, this technique provides a readily quantifiable measure of intratumoral hypoxia (14–16). In these experiments, mice with established A431 xenografts were treated with gefitinib or vehicle, and tumors were harvested at day 1 (pretreatment), day 5, and day 8 ($n = 3$ tumors per time point) and evaluated by immunostaining for pimonidazole adducts as described above. The percentage of pimonidazole immunostaining of non–necrotic tissue was determined in three tumors per time point. A significant difference was observed in pimonidazole-binding between the control and gefitinib-treated groups that was statistically significant at day 5 (control versus gefitinib-treated, 23.1 ± 5.1% versus 6.2 ± 1.1%; $P = 0.005$) and day 8

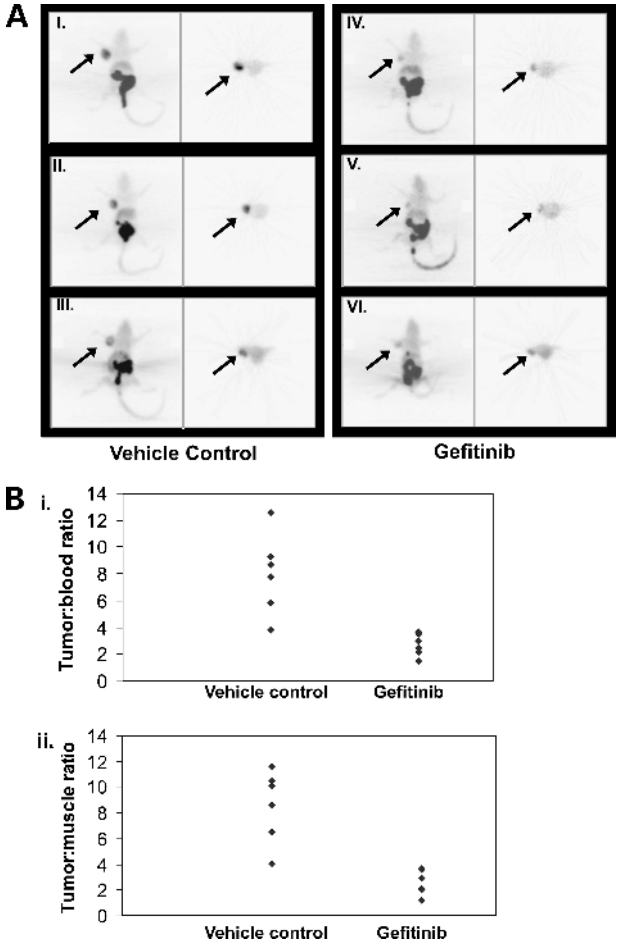

Figure 2. Effect of gefitinib treatment on FAZA uptake in A431 xenografts. **A,** BALB/c nude mice bearing established A431 xenografts were treated with 75 mg/kg/d of gefitinib or vehicle control for 5 d. **A,** FAZA PET imaging was done on mice 3 h after FAZA injection. Representative images are shown from control mice (i, ii, and iii) and from mice treated with gefitinib (iv, v, and vi). *Arrows*, tumors. **B,** following the imaging studies, mice were sacrificed and the tumor to blood (*i*) and tumor to muscle (*ii*) ratios for FAZA uptake were determined (n = 6 per group). A significant reduction was seen for both tumor to blood ratio (P = 0.007) and tumor to muscle ratio (P = 0.002).

(control versus gefitinib-treated, 24.6 ± 5.0 versus 5.2 ± 2.4%; P = 0.003). Interestingly, the gefitinib-treated tumors seemed to contain fewer necrotic areas than their untreated counterparts. In addition, gefitinib-treated tumors showed reduced pimonidazole-binding in comparison with baseline pretreatment levels (day 1, 14.3 ± 1.8%) at both time points examined (day 5, P = 0.003 and day 8, P = 0.006).

In parallel with the pimonidazole binding studies, an additional experiment was conducted where serial FAZA PET imaging was done at day 1 (pretreatment), day 5, and day 8 of a separate cohort of mice with established A431 xenografts treated with gefitinib or vehicle. Representative images of mice treated with vehicle or gefitinib are shown in Fig. 4B. Significantly, the derived tumor to background ratios of FAZA images of mice treated with the same gefitinib schedule correlated strongly with the pimonidazole data (Fig. 4C) providing further experimental validation of the ability of FAZA to mark hypoxia.

Discussion

A number of different strategies have been explored to therapeutically modulate tumor oxygenation. The studies described here show that the epidermal growth factor receptor tyrosine kinase inhibitor gefitinib improves oxygenation within A431 squamous cell carcinoma xenografts. Using *in vivo* PET imaging with the hypoxia marker FAZA, it was seen that treatment with gefitinib reduced hypoxia in A431 xenografts in comparison with untreated control tumors. Importantly, serial PET imaging studies were able to show that gefitinib reduced hypoxia compared with pretreatment levels. These findings were verified in a parallel experiment in which hypoxia was assessed using pimonidazole binding at time points corresponding with the PET studies.

In vivo imaging of hypoxia was conducted using the PET hypoxia imaging agent FAZA. This compound displays different physical properties to fluoromisonidazole, in particular, a lower octanol/water partition coefficient, indicating the potential for more rapid diffusion through tissue and faster excretion, which may result in improved imaging properties. FAZA has been shown to be a superior

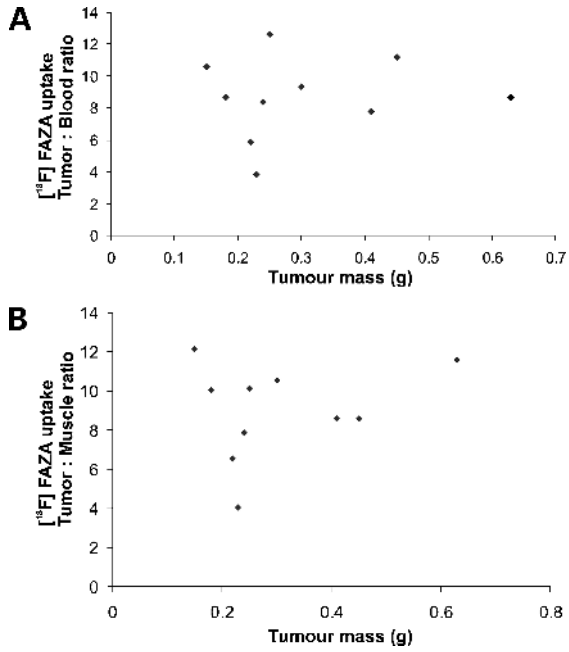

Figure 3. Effect of tumor size on uptake of FAZA in A431 xenografts. The influence of tumor size on uptake of FAZA was evaluated in untreated A431 xenografts of various sizes. Tumor size as reflected by mass (grams) was plotted against (**A**) tumor to blood and (**B**) tumor to muscle ratio of FAZA uptake quantitated *ex vivo.* No correlation was observed between tumor mass and FAZA uptake measured by either tumor to blood ratio (r^2 = 0.01) or tumor to muscle ratio (r^2 = 0.05).

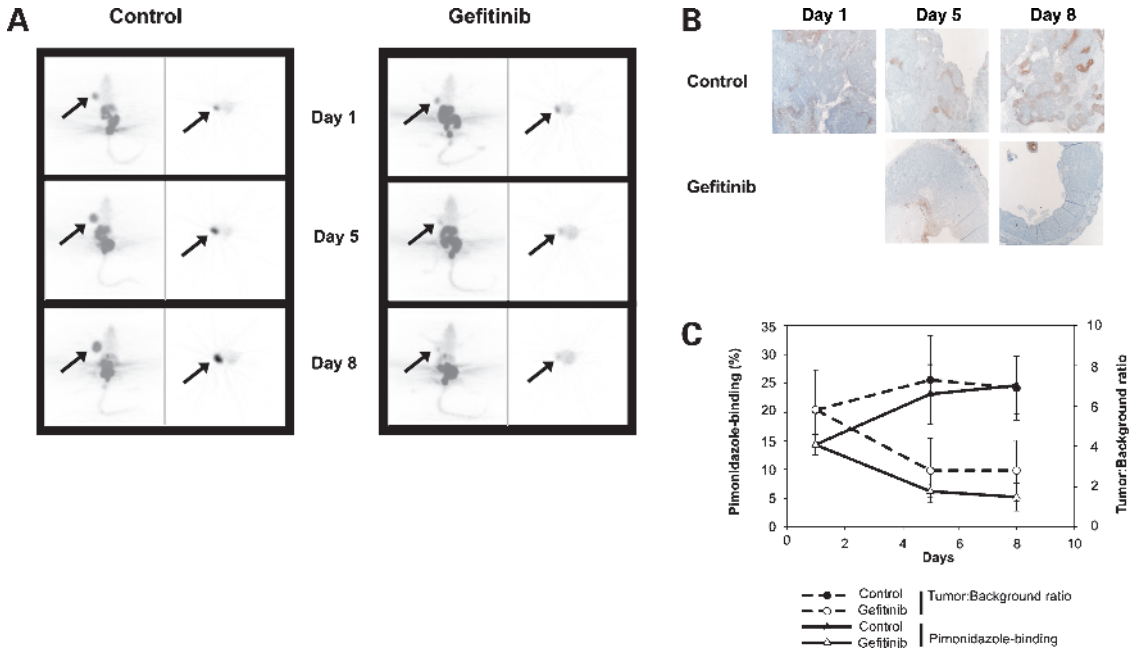

Figure 4. Serial assessment of hypoxia in A431 xenografts using FAZA and pimonidazole binding. **A,** mice with established A431 xenografts were treated with gefitinib (75 mg/kg/d) or vehicle control for 8 d ($n = 3$ per time point). **A,** immunohistochemistry for pimonidazole adducts in A431 xenografts treated with vehicle or gefitinib at baseline (day 1), day 5, and day 8. The percentage of pimonidazole immunostaining of non–necrotic tumor tissue was quantified as indicated in the text. **B,** in a parallel experiment, serial FAZA small animal PET imaging was done at baseline (day 1) and on day 5, and day 8. Representative images (projection and transaxial images) are shown from a control and gefitinib-treated mouse. *Arrows,* tumors. **C,** tumor to background ratios were calculated for the gefitinib-treated and the vehicle-treated mice from the PET images (*points,* mean; *bars,* ± SD from three mice per group). Pimonidazole-binding was quantitated from **A** from $n = 3$ tumors and $n = 2$ or 3 sections per tumor for each data point, and is shown graphically superimposed on the FAZA tumor to background ratios.

imaging agent to fluoromisonidazole in the A431 xenografts studied here (10). However, curiously, in a Walker 256 rat sarcoma model, fluoromisonidazole displayed a superior tumor to background ratio to FAZA (17). Studies of FAZA in humans have shown encouraging results.[5]

A significant strength of the strategy for hypoxia assessment used is that small animal PET imaging technology enabled the performance of serial studies in mice, allowing each tumor to serve as its own control. Moreover, the PET imaging was of sufficient resolution to enable both quantitative and qualitative assessments of hypoxia in the tumors in mice. This allowed detailed comparisons not only between gefitinib-treated and untreated tumors, but also comparisons in individual tumors before and after gefitinib. In addition, a second methodology was used to assess hypoxia, i.e., immunohistochemical assessment of pimonidazole binding. Good correlation was observed between the PET imaging and pimonidazole binding. Of note, polarographic oxygen electrode measurements were not made given the well-described technical limitations of oxygen electrodes, and importantly, from the inability of this technique to distinguish between tumor and necrotic tissue (18, 19). The latter is likely to be important in human tumors such as squamous cell carcinomas that frequently contain large areas of necrosis.

Modulation of intratumoral oxygenation represents a potentially important consequence of gefitinib treatment with implications for combinatorial strategies of gefitinib and radiation. Recently, gefitinib was shown to mediate a similar improvement in tumor oxygenation in two ErbB2-expressing breast cancer xenograft models as measured by flow cytometric analyses of cellular binding of the hypoxia marker EF5 (20), suggesting that the oxygen-modulating effects of the epidermal growth factor receptor inhibitor extends beyond the A431 tumors examined in the current study.

The precise mechanisms by which gefitinib improves tumor oxygenation remain to be established. Gefitinib has been shown to have direct and indirect antiangiogenic effects mediated through the inhibition of production of vascular endothelial growth factors and other proangiogenic proteins (21). Importantly, we have previously shown that gefitinib reduces the production of vascular endothelial growth factor and the vascularity of A431 xenografts (8). Although perhaps counterintuitive, this antiangiogenic action may function to normalize the irregular dysfunctional vasculature present in tumors, thereby improving perfusion and oxygen delivery (22). Another mechanism,

[5] R. J. Hicks, unpublished.

which may occur in parallel, is reduction of oxygen consumption by tumor cells. The use of *in vivo* molecular imaging techniques such as small animal PET scanning or dynamic contrast enhanced magnetic resonance imaging may help to further elucidate the pathophysiologic and biochemical basis of action of gefitinib and other novel anticancer agents.

Acknowledgments

Dr. Piyush Kumar, University of Alberta, provided the FAZA radiolabeling precursor. The authors wish to acknowledge the expert technical assistance of Susan Jackson, Leigh Mathieson, and Donna Dorow.

References

1. Hockel M, Vaupel P. Tumor hypoxia: definitions and current clinical, biologic, and molecular aspects. J Natl Cancer Inst 2001;93:266 – 76.

2. Brown JM. The hypoxic cell: a target for selective cancer therapy—18th Bruce F. Cain Memorial Award Lecture. Cancer Res 1999;59:5863 – 70.

3. Gray LH, Conger AD, Ebert M, Hornsey S, Scott OC. Concentration of oxygen dissolved in tissues at the time of irradiation as a factor in radiotherapy. Br J Radiol 1953;26:638 – 48.

4. Wakeling AE, Guy SP, Woodburn JR, et al. ZD1839 (Iressa): an orally active inhibitor of epidermal growth factor signaling with potential for cancer therapy. Cancer Res 2002;62:5749 – 54.

5. Blackledge G, Averbuch S. Gefitinib ('Iressa', ZD1839) and new epidermal growth factor receptor inhibitors. Br J Cancer 2004;90:566 – 72.

6. Bianco C, Tortora G, Bianco R, et al. Enhancement of antitumor activity of ionizing radiation by combined treatment with the selective epidermal growth factor receptor-tyrosine kinase inhibitor ZD1839 (Iressa). Clin Cancer Res 2002;8:3250 – 8.

7. Huang SM, Li J, Armstrong EA, Harari PM. Modulation of radiation response and tumor-induced angiogenesis after epidermal growth factor receptor inhibition by ZD1839 (Iressa). Cancer Res 2002;62:4300 – 6.

8. Solomon B, Hagekyriakou J, Trivett MK, Stacker SA, McArthur GA, Cullinane C. EGFR blockade with ZD1839 (''Iressa'') potentiates the antitumor effects of single and multiple fractions of ionizing radiation in human A431 squamous cell carcinoma. Int J Radiat Oncol Biol Phys 2003; 55:713 – 23.

9. Williams KJ, Telfer BA, Stratford IJ, Wedge SR. ZD1839 ('Iressa'), a specific oral epidermal growth factor receptor-tyrosine kinase inhibitor, potentiates radiotherapy in a human colorectal cancer xenograft model. Br J Cancer 2002;86:1157 – 61.

10. Piert M, Machulla HJ, Picchio M, et al. Hypoxia-specific tumor imaging with 18F-fluoroazomycin arabinoside. J Nucl Med 2005;46:106 – 13.

11. Reischl G, Ehrlichmann W, Bieg C, et al. Preparation of the hypoxia imaging PET tracer [(18)F]FAZA: reaction parameters and automation. Appl Radiat Isot 2005;62:897 – 901.

12. Surti S, Karp JS. Design evaluation of A-PET: a high sensitivity animal PET camera. Trans Nucl Sci 2003;50:1357 – 63.

13. Arteel GE, Thurman RG, Yates JM, Raleigh JA. Evidence that hypoxia markers detect oxygen gradients in liver: pimonidazole and retrograde perfusion of rat liver. Br J Cancer 1995;72:889 – 95.

14. Raleigh J, Calkins-Adams D, Rinker L, et al. Hypoxia and vascular endothelial growth factor expression in human squamous cell carcinomas using pimonidazole as a hypoxia marker. Cancer Res 1998;58: 3765 – 8.

15. Raleigh JA, Chou SC, Calkins-Adams DP, Ballenger CA, Novotny DB, Varia MA. A clinical study of hypoxia and metallothionein protein expression in squamous cell carcinomas. Clin Cancer Res 2000;6:855 – 62.

16. Varia MA, Calkins-Adams DP, Rinker LH, et al. Pimonidazole: a novel hypoxia marker for complementary study of tumor hypoxia and cell proliferation in cervical carcinoma. Gynecol Oncol 1998;71:270 – 7.

17. Sorger D, Patt M, Kumar P, et al. [18F]Fluoroazomycinarabinofuranoside (18FAZA) and [18F]fluoromisonidazole (18FMISO): a comparative study of their selective uptake in hypoxic cells and PET imaging in experimental rat tumors. Nucl Med Biol 2003;30:317 – 26.

18. Khalil AA, Horsman MR, Overgaard J. The importance of determining necrotic fraction when studying the effect of tumour volume on tissue oxygenation. Acta Oncol 1995;34:297 – 300.

19. Jenkins WT, Evans SM, Koch CJ. Hypoxia and necrosis in rat 9L glioma and Morris 7777 hepatoma tumors: comparative measurements using EF5 binding and the Eppendorf needle electrode. Int J Radiat Oncol Biol Phys 2000;46:1005 – 17.

20. Warburton C, Dragowska WH, Gelmon K, et al. Treatment of HER-2/neu overexpressing breast cancer xenograft models with trastuzumab (Herceptin) and gefitinib (ZD1839): drug combination effects on tumor growth, HER-2/neu and epidermal growth factor receptor expression, and viable hypoxic cell fraction. Clin Cancer Res 2004;10:2512 – 24.

21. Hirata A, Ogawa S, Kometani T, et al. ZD1839 (Iressa) induces antiangiogenic effects through inhibition of epidermal growth factor receptor tyrosine kinase. Cancer Res 2002;62:2554 – 60.

22. Jain RK. Normalization of tumor vasculature: an emerging concept in antiangiogenic therapy. Science 2005;307:58 – 62.